Identification of Time Delay in Pointing Tasks for Human-Blimp Interactions

Tianfu Wu
Department of Electronic and Computer Engineering
Hong Kong University of Science and Technology
Hong Kong, China
0000-0001-7683-777X

Wugang Meng
Department of Electronic and Computer Engineering
Hong Kong University of Science and Technology
Hong Kong, China
0000-0003-4289-2409

Sungjin Cho
Department of Electronic Engineering
Sunchon National University
Suncheon, South Korea
0000-0002-5694-310X

Fumin Zhang
Department of Electronic and Computer Engineering
Department of Mechanical and Aerospace Engineering
Hong Kong University of Science and Technology
Hong Kong, China
0000-0003-0053-4224

2024 9th International Conference on Automation, Control and Robotics Engineering (CACRE) | 979-8-3503-5030-2/24/$31.00 ©2024 IEEE | DOI: 10.1109/CACRE62362.2024.10635018

***Abstract*—In this paper, we explore the problem of estimating time delay parameters when humans interact with a Miniature Autonomous Blimp (MAB). As our earlier research has shown, the Vector Integration to Endpoint (VITE) model can be applied as a reset controller to efficiently minimize the blimp's motion overshoot and mimic the wand motions produced when people interact with it. Furthermore, our study shows that the closed-loop human-blimp dynamics are exponentially stable. However, dealing with the perceptual delay between the operator and the autonomous system is a key challenge in human-robot interaction experiments. In this paper, we use both experimental measurements and the Padé approximation method to model the time delay in human-blimp interactions. Through experiments, we estimate the parameters of the new VITE model after incorporating the time delay. We also demonstrate that the new VITE model remains effective for simulating human-blimp interactions in 3D space, and that human intentions can be inferred from the trajectories of the blimp and pointer movements.**

***Index Terms*—Human robot interaction, indoor miniature blimp, VITE model, time delays**

I. Introduction

The latest advancements in robotics technology have propelled the rapid development of unmanned aerial vehicles (UAVs). With the increasing popularity of drones in both industry and everyday life, collaboration between humans and UAVs is quickly becoming inevitable. Hence, research on human-robot interaction has garnered significant interest in recent years. Quadrotor UAVs stand out as one of the most favored robotic platforms within the realm of 3D HRI research [1]. Individuals can direct quadrotor UAVs to perform particular tasks using various means such as language/voice commands, visual cues, gestures, and other methods [2]. Furthermore, alternative drone models like fixed-wing drones have also been engineered to engage with humans.

However, existing UAVs are still lacking in safety and endurance [3]–[5]. To address this, we developed the Miniature Autonomous Blimp (MAB), a lighter-than-air robot designed for indoor human habitats. The MAB features a helium-filled spherical airbag with an attached gondola [6]. Its soft airbag shell provides natural cushioning, posing no safety threat to humans. Additionally, the buoyancy from the airbag allows the blimp to remain aloft without continuous propulsion, significantly extending its endurance compared to other aerial robots. This makes MAB ideal for HRI experiments that require close human proximity and prolonged aerial suspension.

In our earlier research [7], [8], we investigated the feasibility of utilizing pointing motion control for directing MAB flight. Human pointing motion serves as a simpler and more intuitive user interface. We have applied the VITE model, originally developed for simulating human movement in computer mouse interactions, to model wand movements. According to our research, the VITE model can function as a reset controller to minimize blimp motion overshoot when controlled by people. Furthermore, we have integrated the VITE model with human pointing motions and provided a stability analysis of the system. However, in our previous study [7], [8], we did not consider the time delay that exists during the interaction between the robot and the operator. These delays affect the control performance and may lead to instability in the robot's motion [9], especially when the delays are large relative to the velocity of the robot dynamics.

In this paper, we will analyze the effect of time delay in human operators manipulating a blimp through pointing motions. We show that the VITE model's closed-loop dynamics remain asymptotically stable with the inclusion of the time delay parameter. We perform parameter identification for the new VITE model and experimentally demonstrate its effectiveness in simulating human intentions.

The rest of the paper is organized as follows. Section II presents the relevant background of the study, while Section III formulates the problem. Section IV provides the stability analysis. Section V examines and discusses the experimental results. Finally, Section VI outlines the conclusion and future work.

II. Background

A. VITE Model

For human pointing motion, the VITE model is a second-order dynamic model [10]. This model addresses a human's control over the position of a pointing device which manipulates a visible pointer on a screen. It assumes that the individual aims to move the pointer to a target position.In this context, $y(t)$ denotes the user's control over the pointing device's position, $u(t)$ represents the pointer's perceived position, and r_t indicates the pointer's target position. The difference between the intended target location and the visible pointer position is thus represented by the vector $r_t - u(t)$. The movement of the pointing device is described by the VITE model as:

$$\begin{cases} \dot{\eta}(t) = \gamma\left(-\eta(t) + r_t - u(t)\right) \\ \dot{y}(t) = g\left[\eta(t)\right]_d^+ \end{cases} \tag{1}$$

Here, $\eta(t)$ represents the internal state that explains how a person perceives the difference between the target and pointer positions, integrating all difference vectors over time with a constant gain γ. The pointing action is stopped when the pointer overshoots its destination via the operator $[\cdot]_d^+$. The following equation defines it:

$$[v]_d^+ = \begin{cases} v, & \text{if } \langle v, d\rangle \geq 0 \\ 0, & \text{otherwise} \end{cases} \tag{2}$$

The path from the pointer to the target position at the beginning instant is the direction that d describes here. The go signal, g, a feedback gain, indicates the movement of the pointer according to the internal state $\eta(t)$. The blimp system uses the wand locations as inputs, and the operator's pointing duty is treated as a feedback mechanism. The output that will be adjusted to the desired position is the blimp position. This is thought to be an output regulation problem with the controller design. The VITE model is seen as a feedback control law that uses the difference vector $r_t - u(t)$ to produce the wand altitude $y(t)$. By adjusting the wand altitude $y(t)$, human operator will drive the blimp's height $u(t)$ to the goal altitude r_t.

Fig. 1. Human-Blimp Interaction

B. Delay Estimation

We investigate the problem of time delays in the interaction between the blimp and the human operator in this paper. Specifically, there are two primary types of delays within the system: the delay between the operator's movement of a wand and the blimp's recognition of this movement, and the time delay for an operator to sense the movement of a blimp and determine whether the blimp has arrived at a target position.

For the time delay of human perception of blimp motion, the response delay of human perception is measured experimentally due to its difficulty. In order to accurately simulate this delay, we use the Pade approximation method [11], [12] and introduce a first order linear differential equation to describe the dynamic behavior of this system. Here, $\hat{u}$ represents the operator's perceived vertical position of the blimp, u indicates the actual altitude of the blimp, and τ_1 is the time constant for the perception delay. This equation models the rate of change of the perceived height $\hat{u}$ through a decay term defined by τ_1 and a term driven by the actual blimp height u.

$$\dot{\hat{u}} = -\frac{1}{\tau_1}\hat{u} + \frac{1}{\tau_1}u \tag{3}$$

Meanwhile, the delay in the blimp's response to the movement of the magic wand is primarily composed of two parts: the OptiTrack system's internal processing time to determine the blimp's position and broadcast the data, and the communication delay in transmitting control commands from the ground station to the blimp. Figure 2 illustrates the process by which the blimp acquires the position of the wand.

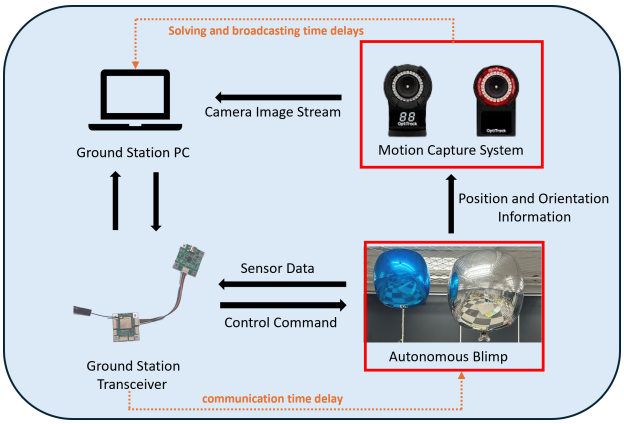

Fig. 2. Communication Process

Thus, τ_2 can be expressed by the following equation:

$$\tau_2 = T_{OptiTrack} + T_{Comm} \tag{4}$$

And We calculate the delay in signal transmission by consulting the Optitrack manual and by recording the timestamp of the message transmission.

III. Problem Formulation

We explore human pointing movements when interacting with a miniature autonomous blimp, as shown in figure 1.

The operator moves a wand with a marking while observing the location of the blimp. And the operator controls the blimp toward an unknown target in the vertical direction. A series of experiments are conducted to collect data on the movement of the wand and the blimp.

In order to simplify the dynamics model, we adopt the presumption from previous studies that the human-specified horizontally oriented location position of the target aligns with the blimp's horizontal location. Under this assumption, let $y(t)$ represent the wand's vertical position, $u(t)$ denote the blimp's height, and $r(t)$ indicate the target's vertical position. Our approach involves using the VITE model to simulate human pointing actions.

We assume that when a human operator interacts with the blimp [7], the motion of the wand can be modeled in the following figure.

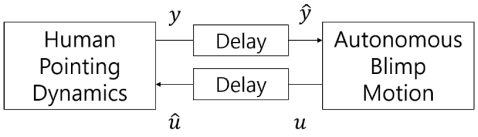

Fig. 3. Closed Loop of Human-Blimp Interacting Motion

The human operator aims to direct the blimp's motion towards the desired location by using the wand. Since the blimp has its own altitude control loop that allows it to follow the movement of the wand, this is the reason why the operator is able to control the movement of the blimp by moving the wand with markers. In our previous study [8], we experimentally collected the real-time corresponding positions of the wand position and the blimp, and identified the parameters of the VITE model using global optimization techniques.

Latency in human-blimp interaction experiments has not been sufficiently emphasized in previous research [8]. Specifically, there are two main types of delays between human pointing dynamics and autonomous blimp motion. TThe first kind is the interval of time between the wand's actual movement and its identification of the position of the blimp. The second type is the time difference between the blimp's movement and the human eye's observation of the blimp's position. Both types are time-varying communication delays, which can lead to instability in the operator's system for interacting with the blimp, causing control issues and affecting experiment accuracy and validity. This paper's primary contribution is the systematic incorporation of these two delay parameters into the VITE model for the first time. By adjusting the model parameters to reflect these delay effects, we significantly improve system stability and response accuracy. This approach better simulates and optimizes the dynamic behavior during human-computer interaction, providing a more reliable theoretical basis for subsequent research on autonomous control systems.

After taking the time delay into account, the close loop of the human-blimp interaction motion is shown in Figure 3. And the VITE model considering the time delay will be modified to the following equation.

$$\dot{\eta} = \gamma\left(-\eta(t) + r_t - \hat{u}(t)\right). \tag{5}$$

Here, η is internal state, γ is a constant gain, r_t is a desired height, and $\hat{u}(t)$ is a delayed height of the blimp. Combined with our previous research [8], the motion dynamics of the blimp can be expressed as

$$m\ddot{u} + D\dot{u} = K_p(\hat{y}(t) - u(t)). \tag{6}$$

In this paper, we consider the effect of time delay while analyzing the stability of a dynamical system consisting of human pointing motions and blimp dynamics. We identify the parameters of the VITE model by recording multiple sets of data on the motion of the wand and the blimp. The unknown reference target location r_t, the gains g and γ, and the operator's perceived movement timeτ_1 are all included in the parameters of the VITE model.Last but not least, we also take an actual experiment to measure the delay of the blimp to perceive the movement of the wand τ_2

IV. Stability analysis

In this session, we demonstrate that the closed-loop dynamics and blimp dynamics, as described by the VITE model with consideration of time delay, are asymptotically stable. The target height is assumed to be at the origin, and the blimp's starting height is underneath the desired height. A comprehensive clarification and rationale for changing the assumptions is provided in our previous study [7]. Based on equations (3),(4) and (5) we constructed the following equation of state for the motion of the human- blimp interaction including the delay.Let x be a state variable representing $[x_1\, x_2\, x_3\, x_4\, x_5\, x_6] \triangleq [u\, \hat{u}\, \eta\, \dot{u}\, y\, \hat{y}]$.Then

$$\mathbf{x} = \begin{bmatrix} x_4 \\ -\frac{1}{\tau_2}x_2 + \frac{1}{\tau_2}x_1 \\ -\gamma\left(x_3 + x_2\right) \\ -\frac{D}{m}x_4 + K_p\left(x_6 - x_1\right) \\ g x_3^+ \\ -\frac{1}{\tau_1}x_6 + \frac{1}{\tau_1}x_5 \end{bmatrix}, \tag{7}$$

Where $x_3^+ = x_3$ when $x_3 \geq 0$, and $x_3^+ = 0$ when $x_3 < 0$. The equilibrium set denoting E is $\{x_4 = 0, x_1 = x_2 = -x_3 = x_6 = x_5, x_3 \leq 0\}$. We analyze the stability according to x_3. Let $\mathbf{z}$ be $\left[x_2 - x_1\ x_3 + x_2\ x_6 - x_1\ x_6 - x_5\ x_4\ x_3^+\right]$. When $x_3 \geq 0$,

$$\dot{\mathbf{z}} = \begin{bmatrix} -\frac{1}{\tau_2} & 0 & 0 & 0 & 0 & -1 \\ -\frac{1}{\tau_2} & 0 & -\gamma & 0 & 0 & 0 \\ 0 & 0 & 0 & -\frac{1}{\tau_1} & -1 & 0 \\ 0 & 0 & 0 & -\frac{1}{\tau_1} & 0 & -g \\ 0 & 0 & \frac{K_p}{m} & 0 & -\frac{D}{m} & 0 \\ 0 & -\gamma & 0 & 0 & 0 & 0 \end{bmatrix} \mathbf{z} = A_1\mathbf{z}. \tag{8}$$

When $x_3 < 0$,

$$\dot{\mathbf{z}} = \begin{bmatrix} -\frac{1}{\tau_2} & 0 & 0 & 0 & -1 & 0 \\ -\frac{1}{\tau_2} & 0 & -\gamma & 0 & 0 & 0 \\ 0 & 0 & 0 & -\frac{1}{\tau_1} & -1 & 0 \\ 0 & 0 & 0 & -\frac{1}{\tau_1} & 0 & -g \\ 0 & 0 & \frac{K_p}{m} & 0 & -\frac{D}{m} & 0 \\ 0 & -\gamma & 0 & 0 & 0 & 0 \end{bmatrix} \mathbf{z} = A_2\mathbf{z}. \quad (9)$$

The closed loop system is exponentially stable when Routh stability criteria is satisfied with λ-polynomial derived from $\det(\lambda I - A_1) = 0$. Let $a_1, a_2, a_3, a_4, a_5, a_6$ are coefficients of $\lambda^6 + a_1\lambda^5 + a_2\lambda^4 + a_3\lambda^3 + a_4\lambda^2 + a_5\lambda + a_6 = 0$. Then,

$$\begin{cases} a_1 = \dfrac{D}{m} + \dfrac{1}{\tau_1} + \dfrac{1}{\tau_2} + \gamma \\ a_2 = \dfrac{K_p}{m} + \dfrac{D}{m}\left(\dfrac{1}{\tau_1} + \dfrac{1}{\tau_2} + \gamma\right) \\ \qquad + \dfrac{1}{\tau_1\tau_2} + \left(\dfrac{1}{\tau_1} + \dfrac{1}{\tau_2}\right)\gamma \\ a_3 = \dfrac{K_p}{m}\left(\dfrac{1}{\tau_1} + \dfrac{1}{\tau_2} + \gamma\right) \\ \qquad + \dfrac{D}{m}\left(\dfrac{1}{\tau_1\tau_2} + \left(\dfrac{1}{\tau_1} + \dfrac{1}{\tau_2}\right)\gamma\right) + \dfrac{\gamma}{\tau_1\tau_2} \\ a_4 = \dfrac{K_p}{m}\left(\dfrac{1}{\tau_1\tau_2} + \left(\dfrac{1}{\tau_1} + \dfrac{1}{\tau_2}\right)\gamma\right) + \dfrac{\gamma D}{m\tau_1\tau_2} \\ a_5 = \dfrac{K_p\gamma}{m\tau_1\tau_2} \\ a_6 = \dfrac{K_p g\gamma}{m\tau_1\tau_2} \end{cases} \quad (10)$$

If the first column of Routh table has all the positive values, the system is exponentially stable. The first column is composed of $a_1, b_1, c_1, d_1, e_1, f_1$ where

$$\begin{cases} b_1 = \dfrac{a_1a_2 - a_3}{a_1} \\ c_1 = \dfrac{a_3b_1 - a_1b_2}{b_1} \\ d_1 = \dfrac{b_2c_1 - c_2b_1}{c_1} \\ e_1 = \dfrac{d_1c_2 - d_2c_1}{d_1} \\ f_1 = a_6 \\ b_2 = \dfrac{a_1a_4 - a_5}{a_1} \\ b_3 = d_2 = a_6 \\ c_2 = \dfrac{a_5b_1 - a_1b_3}{b_1} \end{cases} \quad (11)$$

Similarly, we demonstrate the exponential stability of equation (9). We proved the stability of blimp-human interaction systems, which are comprised of the VITE model and the blimp dynamics, in our earlier research [7], [8]. To guarantee the stability of the interaction dynamics between the blimp and the human operator, we employ the same experimental setup in this paper.

V. Experiment Results

A. Experimental Setup

In our experiments, the operator uses a wand to move the blimp between two target locations at different heights, repeating the process for 100 seconds with vertical movement only. The experiment was conducted at the flying field using an OptiTrack motion capture system. Reflective markers on the blimp and wand tracked their positions. The blimp started about 1 m from the operator at a height of 1.5 m, with target heights between 0.5 m and 2 m. Figure 4 shows the experimental setup.

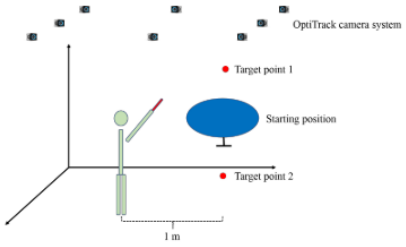

Fig. 4. Experiment setup,blimp and operator maintain 1m distance.

B. Data Processing

Previous research has demonstrated that there is noise [13] in the pointer velocity data when humans perform pointing motions. The noise is shown in the following figure 5. Therefore, to address this problem, we use a Savitzky-Golay filter with a fourth-order polynomial to filter the wand velocities and compute smooth wand trajectories by integrating over the filtered wand velocity data. Here we denote the smoothed wand trajectory as $\tilde{y}(t)$.

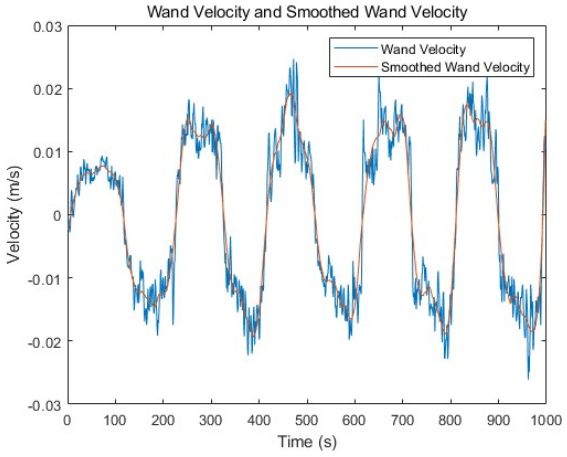

Fig. 5. Noise in velocity

Regarding the wand's movement trajectory, the method is the same as in the preceding one. We separate the upward and downward motions in the filtered wand trajectory $\tilde{y}(t)$ into many segments. A trial is considered complete once the human stops changing the height of the wand, indicating satisfaction with the blimp's height. The time interval of the experiment may thus be split into $[T_1^-, T_1^+], [T_2^-, T_2^+], \ldots, [T_N^-, T_N^+]$, which correspond to the up and down motions of the wand. T_n^- and T_n^+ denote the beginning and finishing timings of the n-th trial, respectively, and $T_{n-1}^+ = T_n^-$. The wand stops moving at the conclusion of each trial, as indicated by $\dot{y}(t) = 0$. In each experimental dataset, we exclude incomplete trial data points. Figure 6 illustrates a set of blimp and wand trajectories.

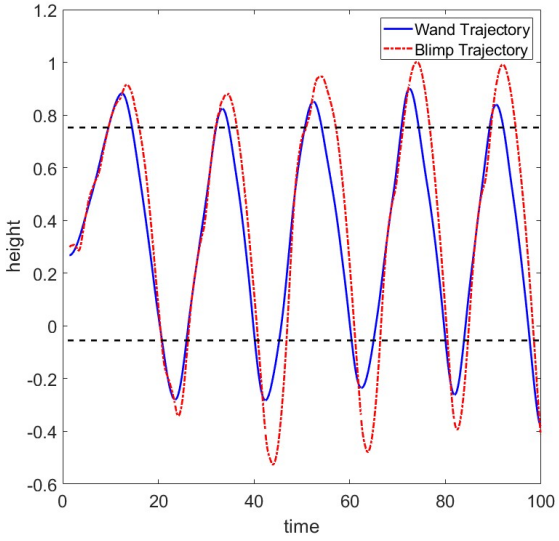

Fig. 6. Blimp and Wand trajectory.

C. Measurement of Communication Delays

By reviewing the Optitrack product manual with the actual recording of the delay output on the operating software of the Optitrack system, it can be inferred that the motion capture system takes around 1.1 ms in total to calculate the blimp's altitude and send it to the ground PC during the pointing motion delay. Meanwhile, we derive the communication time delay in Fig. 2 by simultaneously recording the time stamps of the string sent by the ground station and the string received by the blimp.When recording the timestamps, we maintain a distance of approximately 1 meter between the ground station and the blimp. By continuously sending data strings from the ground station to the blimp and recording the timestamps of both sending and receiving events, we measure the communication delay. The average delay between the ground station and the blimp is approximately 11.9 ms. Therefore,$\tau_2 = T_{\text{OptiTrack}} + T_{\text{Comm}} = 13ms$

D. Parameter Idtification

The set of all upward sections is represented by $\Omega_u = \{n \in \mathbb{Z} \mid \dot{\tilde{y}}(t) > 0, t \in [T_n^-, T_n^+]\}$ and the set of downward sections is represented by $\Omega_d = \{n \in \mathbb{Z} \mid \dot{\tilde{y}}(t) < 0, t \in [T_n^-, T_n^+]\}$. Let $r_{t,u}$ and $r_{t,d}$ denote the target positions for the upward and downward sections, respectively. The set of unknown parameters in the VITE model is denoted as $\Phi = \{\hat{g}, \hat{\gamma}, \hat{r}_{t,u}, \hat{r}_{t,d}, \tau_1\}$. The following initial value problem may be used to create a simulated wand trajectory $y^*(t)$ where the real blimp trajectory $u(t)$ from the experiment and a set of parameters Φ are used to simulate the wand trajectory via the VITE model. Additionally, since the human stops moving the wand at the start and end of each segment, the internal state must be zero at those points. The following equations can be derived based on these requirements.

$$\begin{cases} \dot{\hat{\eta}}(t) = \begin{cases} \hat{\gamma}(-\hat{\eta}(t) + \hat{r}_{t,u} - \hat{u}(t)), & \text{if } n \in \Omega_u \\ \hat{\gamma}(-\hat{\eta}(t) + \hat{r}_{t,d} - \hat{u}(t)), & \text{if } n \in \Omega_d \end{cases} \\ \dot{y^*}(t) = \hat{g}[\hat{\eta}(t)]_d^+ \\ y^*(0) = \tilde{y}(0) \\ \hat{\eta}(T_n^-) = 0,\ n \in \Omega_u \cup \Omega_d \\ \dot{\hat{u}}(t) = -\dfrac{1}{\tau_1}\hat{u}(t) + \dfrac{1}{\tau_1}u(t) \end{cases} \tag{12}$$

We define the problem of parameter identification as a problem of residual optimization where the objective is to mreduce the discrepancy between the reconstructed wand trajectory and the filtered smooth wand trajectory. To solve this problem, we change the terminal restriction when the human internal state is zero to a penalty term in the cost function, which is similar with previous studies. The equation is formulated as follows.

$$\min_{\Phi} \left(\sum_{n \in \Omega_u} \int_{T_n^-}^{T_n^+} (\tilde{y}(t) - y^*(t))^2 dt + \sum_{n \in \Omega_d} \int_{T_n^-}^{T_n^+} (\tilde{y}(t) - y^*(t))^2 dt + \beta \sum_{n \in \Omega_u \cup \Omega_d} \hat{\eta}(T_n^+)^2 \right)$$

s.t.

$$\begin{cases} \dot{\hat{\eta}}(t) = \begin{cases} \hat{\gamma}(-\hat{\eta}(t) + \hat{r}_{t,u} - \hat{u}(t)), & \text{if } n \in \Omega_u \\ \hat{\gamma}(-\hat{\eta}(t) + \hat{r}_{t,d} - \hat{u}(t)), & \text{if } n \in \Omega_d \end{cases} \\ \dot{y^*}(t) = \hat{g}[\hat{\eta}(t)]_d^+ \\ y^*(0) = \tilde{y}(0) \\ \hat{\eta}(T_n^-) = 0, \qquad n \in \Omega_u \cup \Omega_d \\ \dot{\hat{u}}(t) = -\dfrac{1}{\tau_1}\hat{u}(t) + \dfrac{1}{\tau_1}u(t) \end{cases} \tag{13}$$

E. Results and Discussion

We determined the unknown parameters in the VITE model, such as the go signal, time delay parameters, target position, and feedback gain, based on the data gathered. Figure 7 shows the results of the experiment.The identified target positions of the blimp are 0.8106 m and -0.11 m. Meanwhile, the feedback gain γ is 0.518, the go signal value is 0.1818, and the time delay parameter, τ_1 for the human operator to judge the position of the blimp is $\frac{1}{23.3789} \approx 42.77$ ms .

We evaluate the performance of parameter identification by comparing the experimentally measured wand trajectories with those

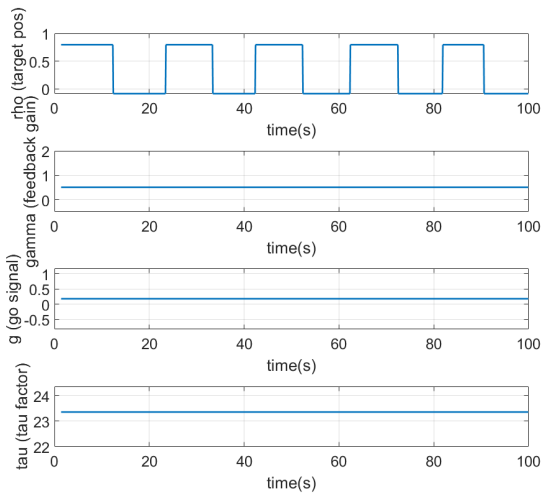

Fig. 7. Parameter identification results

simulated using the VITE model. The difference in the simulated and real wand trajectories' root mean square error (RMSE) is 0.0906m, or around 8.4% of the overall variation in height that occurred during the entire experiment. Figure 8 shows a comparison of wand trajectories reconstructed through the VITE model with real measured wand trajectories. This finding highlights that the VITE model, which incorporates a time delay factor, not only accurately replicates the actual trajectory of the wand but also adeptly captures the nuances of human intent. This demonstrates the model's robustness and reliability in modeling complex human motions. By integrating the time delay factor, the model aligns closely with real-world behaviors, ensuring a precise and insightful representation of human actions.

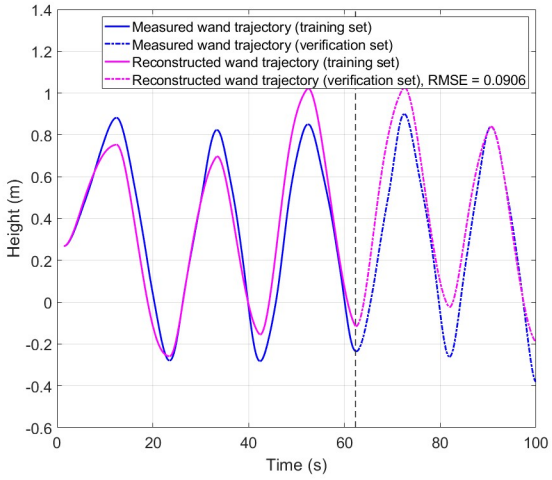

Fig. 8. Comparison of the simulated and measured wand trajectory

VI. Conclusion

We identify the VITE parameter that accounts for time delay by recording data from humans controlling the movement of a blimp through pointing motions. Our results demonstrate that the entire human-blimp interaction system remains stable despite the inclusion of the time delay. Additionally, the VITE model, with the incorporated time delay parameter, continues to accurately simulate human behavior in human-blimp interactions. In our future work, we will enhance the experimental methodology to ensure that the reconstructed wand motion curves from the VITE model more accurately reflect real motion. Additionally, we aim to design interaction controllers with improved performance.

References

[1] N. Yao, Q. Tao, W. Liu, Z. Liu, Y. Tian, P.-y. Wang, T. Li, and F. Zhang, "Autonomous flying blimp interaction with human in an indoor space," *Frontiers of Information Technology Electronic Engineering*, vol. 20, pp. 45–59, 01 2019.

[2] D. Szafir, B. Mutlu, and T. Fong, "Communicating directionality in flying robots," in *2015 10th ACM/IEEE International Conference on Human-Robot Interaction (HRI)*, 2015, pp. 19–26.

[3] K. Asadi, A. K. Suresh, A. Ender, S. Gotad, S. Maniyar, S. Anand, M. Noghabaei, K. Han, E. Lobaton, and T. Wu, "An integrated ugv-uav system for construction site data collection," *Automation in Construction*, vol. 112, p. 103068, 2020.

[4] V. Srisamosorn, N. Kuwahara, A. Yamashita, T. Ogata, S. Shirafuji, and J. Ota, "Indoor human face following with environmental fisheye cameras and blimp," *Advanced Robotics*, vol. 34, no. 9, pp. 621–636, 2020.

[5] S. U. Ferdous, A. Mohammadi, and S. Lakshmanan, "Developing a low-cost autonomous blimp with a reduced number of actuators," in *Unmanned Systems Technology XXI*, vol. 11021. SPIE, 2019, pp. 73–80.

[6] Q. Tao, J. Wang, Z. Xu, T. X. Lin, Y. Yuan, and F. Zhang, "Swing-reducing flight control system for an underactuated indoor miniature autonomous blimp," *IEEE/ASME Transactions on Mechatronics*, vol. 26, no. 4, pp. 1895–1904, 2021.

[7] M. Hou, Q. Tao, P. Varnell, and F. Zhang, "Modeling pointing tasks in human-blimp interactions," in *2019 IEEE Conference on Control Technology and Applications (CCTA)*. IEEE, 2019, pp. 73–78.

[8] M. Hou, Q. Tao, and F. Zhang, "Human pointing motion during interaction with an autonomous blimp," *Scientific Reports*, vol. 12, no. 1, p. 11402, 2022.

[9] P. Varnell and F. Zhang, "Dissipativity-based teleoperation with time-varying communication delays," *IFAC Proceedings Volumes*, vol. 46, no. 27, pp. 369–376, 2013.

[10] D. Bullock and S. Grossberg, "Neural dynamics of planned arm movements: emergent invariants and speed-accuracy properties during trajectory formation." *Psychological review*, vol. 95, no. 1, p. 49, 1988.

[11] N. S. Nise, *Control systems engineering*. John Wiley & Sons, 2020.

[12] S. Cho, Q. Tao, P. Varnell, S. Maxon, and F. Zhang, "Autopilot design of a class of miniature autonomous blimps enabled by switched controllers," *International Journal of Intelligent Robotics and Applications*, vol. 6, no. 3, pp. 385–396, 2022.

[13] J. Müller, "Dynamics of pointing with pointer acceleration," *Human-Computer Interaction*, vol. INTERACT 2017: 16th IFIP TC 13 International Conference, Mumbai, India, September 25–29, 2017, Proceedings, Part III 16, pp. 475–495, 2017.